J Musculoskelet Neuronal Interact 2012; 12(3):155-164

Original Article

Hylonome

# Peripheral QCT sector analysis reveals early exercise-induced increases in tibial bone mineral density

**R.K. Evans[1], C.H. Negus[2], A.J. Centi[1], B.A. Spiering[3], W.J. Kraemer[4], B.C. Nindl[1]**

[1]U.S. Army Research Institute of Environmental Medicine, Natick, MA; [2]L-3 ATI, Simulation, Engineering, and Testing, San Diego, CA; [3]Department of Kinesiology, California State University, Fullerton, CA; [4]University of Connecticut, Storrs, CT

## Abstract

**Objectives:** The purpose of this controlled trial was to determine whether subtle changes in mineralization and geometry of the tibia were evident following short term exercise interventions. **Methods:** Fifty-seven female volunteers (age 20.1±1.6) were randomized to one of four, 13-week training groups: sedentary control, resistance training, aerobic training, or combined aerobic-resistance. A pQCT image analysis software was developed and used to analyze images taken at sites 4%, 38% and 66% from the distal tibia at baseline and at completion of training. Parameters of bone mineral density, geometry and strength were determined for the entire scan cross-section and for each of six 60° polar sectors. Repeated-measures ANOVA and Fisher's LSD post hoc tests analyzed the effects of training over time. **Results:** Trabecular density (*TrDn*) at the 4% site increased from 279.8±37.1 to 283.1±36.0 mg/cm$^3$ in the aerobic group, and from 285.1±24.6 to 287.5±22.9 mg/cm$^3$ in the combined group over the study period ($P \leq 0.001$). Regional sector analyses revealed that impact exercises resulted in localized changes to the medial aspect of the tibia. Small increases in total bone area were observed in the diaphysis (38% site) ($P<0.05$). **Conclusions:** Subtle, regional increases in trabecular density may be an early measurable manifestation of bone quality changes.

**Keywords:** pQCT, Exercise, Bone, Early Adaptation, Volumetric Density

## Introduction

The osteogenic effect of exercise training is supported by numerous cross-sectional and intervention studies among a variety of animal[1-4] and human cohorts[5-9]. Observed beneficial changes from long-term exercise training include enhanced mineralization, cortical adaptation, or a combination of both[7,10,11]. Turner and Robling have developed an equation to predict the osteogenic potential of exercise through calculation of an osteogenic index (OI) that takes into account intensity of exercise, the number of loading cycles, and exercise volume[12]. This index was used in a recently published companion paper to determine if the predicted OI of three controlled, periodized 8-week exercise programs was related to changes in serum markers of bone turnover[13]. While there was no consistent relationship between OI and bone turnover, the investigators observed a small but significant increase in volumetric bone mineral density (vBMD) at the distal tibia in cross-sectional images of trabecular bone in the high-impact exercise group. This finding may represent a site-specific adaptation to impact exercise in humans which is discernable earlier than conventionally thought.

Animal studies have demonstrated that there are detectable, site-specific adaptations in both geometry and mineralization following short-term exercise interventions. Evidence suggests that osteogenesis is greatest in the early phase of a loading intervention, with cortical bone formation apparent at the periosteal and endocortical surfaces after just six weeks of loading[1]. Significant gains in total cortical area of the tibial and femoral diaphyses, reflected in increased periosteal perimeter, were observed following as few as 5-20 jumps per day in young rats[2]. Early changes in trabecular bone mass parameters at the proximal tibia have been observed following a six-week program of progressive resistance training in adult

This study was funded in part by a grant from the U.S. Army Medical Research and Materiel Command's Bone Health and Military Medical Readiness Research Program.

*Corresponding author: Charles H. Negus, Ph.D., Sr. Scientist, L-3 ATI, Simulation, Engineering, and Testing, 10770 Wateridge Circle, Suite 200, San Diego, CA 92121*
*E-mail: Charles.Negus@L-3Com.com*

*Edited by: J. Rittweger*
*Accepted 12 July 2012*

rats[3], and after three weeks of treadmill running in young rats[4]. These changes were local, both in terms of site (e.g., epiphyseal vs. diaphyseal), surface (e.g. periosteal vs endosteal), and region (e.g., anterior vs. posterior), with different regimens leading to differing localized effects.

Whether similar site-specific short-term responses are discernable in humans, whose remodeling cycle is longer than small animals, requires a refined analysis of noninvasive images. Peripheral quantitative computed tomography (pQCT) has been validated and used extensively to assess mineralization and geometry parameters of cross-sectional images[14,15]. Exercise-related adaptations of cortical bone area and thickness, periosteal area, and trabecular density have been observed in pQCT images in the dominant arm of tennis players[5,6]. Similar differences in geometry and trabecular density of the lower extremity are evident when comparing the femur and tibia of triple jumpers and matched controls[7]. Recently, pQCT has successfully measured changes in bone parameters resulting from exercise interventions among children[16-19].

In addition to its utility in assessing bone parameters calculated from a whole bone cross-section, pQCT and has recently been used to assess polar-regional measurements in the cortical bone of animals[20] and humans[21], and trabecular bone in humans[22]. Regional analysis of pQCT images of the proximal tibia has also revealed site-specific changes in bone mass following a high-impact exercise intervention combined with hormone replacement therapy in postmenopausal women[23], suggesting that this method may be valuable in detecting early site-specific regional changes in bones of the lower extremity. The authors of this paper recently reported use of a similar analysis technique to assess sector-by-sector differences in bone composition and morphology between male and female members of a military cohort[24].

The purpose of this study was to expand on previous work[13] to determine whether regional changes in bone mineralization and geometry of the tibia were evident in the pQCT images of healthy college-aged women following one of three rigorous exercise interventions with varied osteogenic indices.

## Methods

### *Subjects*

Seventy young, healthy college women were enrolled in this study, which was approved by the United States Army Research Institute of Environmental Medicine (USARIEM), University of Connecticut (UCONN), and Medical Research and Materiel Command (MRMC) Human Subjects Research Review Boards (HSRRB). All volunteers were asked to read and sign an informed consent document prior to participation. Women who were smokers, pregnant, lactating, or participating in physical training activities more than twice per week in the preceding six months were excluded from participation. Additionally, women identified during a medical examination as having any endocrine, orthopedic, menstrual cycle disturbances, or other pathologic processes were excluded. Participants who were taking oral contraceptives were included in the study. Investigators adhered to AR 70-25 and USAMRMC Regulation 70-25 and provisions of 32 CFR Part 219 on the use of volunteers in research.

### *Experimental Design*

All volunteers selected for this study reported exercising fewer than 2 days per week prior to the study. Volunteers participated in testing and training over a 13-week period, 8 of which involved taking part in a supervised training intervention. The 8-week regimen was selected to best allow for the program(s), if effective, to be incorporated into an 8-week military recruit training program. (Please see Tables 1-3 in Lester, et al., 2009[13] for detailed training schedules.) Volunteers were tested for dependent variables of interest at baseline (Pre), after 4 weeks of training (Mid), and after 8 weeks of training (Post), occurring over a total study duration of 13 weeks. Following baseline testing a randomized block procedure, based on entry-level fitness tests, was used to assign qualified participants to one of three exercise groups (aerobic, resistance, or combined training), or a control group. An analysis of variance was performed to ensure the most equal distribution of subjects based on the following descriptive variables (in order of priority): height, weight, bone mineral content, menstrual cycle status, bench press strength, and squat strength.

### *Procedures*

#### Anthropometrics

Height (cm) was measured using a stadiometer, and body mass using a digital scale (kg). Tibial length was measured using a leg length caliper. Measurement was taken from the central point of the medial malleolus to the central point of the medial tibial condyle and recorded in mm.

#### Training Interventions

All training sessions were supervised and individualized according to each volunteer's physical capacities, and were performed on three non-consecutive days each week. Certified strength and conditioning specialists oversaw all training sessions to ensure proper progression and to offer instruction and motivation. The sessions began and ended with a 5-10 minute warm-up and cool-down which included light jogging, calisthenics, and stretching. A detailed description of the aerobic (AER), resistance training (RES) and combined aerobic-resistance training (COM) regimens, to include predicted osteogenic index (OI), are described in a previous publication[13], and are summarized as follows. Volunteers in the AER group performed high-impact aerobic/running-based exercise sessions. Individuals assigned to the RES group followed a nonlinear periodized model in which load and repetition were varied on a daily basis (light, moderate or heavy). The COM aerobic-resistance group performed the entire training regimen of both the AER and RES exercise programs during a single session, with the resistance exercise performed first. Mean weekly OIs were 20.6±2.2 for the AER group (range 15.7-23.6), 16.0±1.9 for the RES group (range 13.4-20.1), and 36.9±5.2 for the COM group (range 27.9-43.9). The CON

group was asked to refrain from participating in any structured exercise program for the duration of the study.

### Peripheral quantitative computed tomography (pQCT)

Peripheral quantitative computed tomography (Stratec Medizintechnik, Pforzheim, Germany XCT 3000) was used to measure bone characteristics of the tibia. To assure measurement quality, a calibration check was performed on each data collection day by scanning a standard phantom with known densities of 168.5, 317.4 and 462.5 mg/cm$^3$. Volunteers were positioned on a chair with the non-dominant leg (as assessed by self-reporting) extended through the scanning cylinder and were asked to maintain a convenient and stable position for the duration of the procedure (10-15 minutes). Initial scout scans were conducted at a scan speed of 40 mm/sec to identify the distal end plate of the tibia. Following this, scans of the tibia (single axial slices of 2.4 mm thickness, voxel size 0.4 mm, measure diameter 140 mm) were taken at a translation speed of 20 mm/s at 4%, 38%, and 66% of the measured tibial length proximal from the distal endplate of the tibia. These sites are typically used to analyze trabecular (4%) and cortical (38% and 66%) bone characteristics of the tibia.

### Image Analysis Procedure

The goal of this study was to assess whether subtle site-specific changes in bone could be visualized following short-term exercise training. For this reason, rather than using the default measures exported from the Stratec pQCT software, we further refined a novel procedure described previously[24] that would allow us to quantify potential changes in density and geometry within sectors. Image sets obtained using pQCT were analyzed using software written in Matlab (MathWorks, Natick, MA) which we called *BAMpack*- the Bone Alignment and Measurement package.

To standardize positioning of the images across all scans the image sets first underwent a rotation and registration procedure. Each 4% slice image was centered on the tibial perimeter. The 38% and 66% slices were centered on the intramedullary canal, as the neutral axis seems better defined by the center of the canal than the center of the periosteal boundary. Improvements to *BAMpack* implemented in this study included new automatic image rotation and alignment algorithms. For most subjects the 10 degree sector (at the 66% scan) with the greatest cortical area was used to consistently define the anterior tibia, though for 4 subjects with thick posterior cortices the images were rotated manually. The 4% and 38% images were then rotated accordingly by the same angle as at 66%. The images from two subjects who had images collected from their right legs were inverted so that they could be compared with the left tibias of the other subjects. Alignment was checked for each subject by overlaying plots of the periosteal boundaries for each subject. The maximum permissible alignment error was verified during a position sensitivity study of cadaveric tibiae (data not shown). Goodness of alignment was determined by comparing the coordinates of registration points on the boundary of the Master image with the Slave image. Distance between Master-Slave registration point pairs was calculated followed by the mean Root Mean Square (RMS) value for all registration pairs. Image sets whose mean RMS alignment error was greater than our alignment threshold are discarded. A later validation study was conducted with 11 cadaveric tibiae in which scans were collected 1 slice thickness (2.5 mm) at, above and below the nominal scan locations of 4%, 38%, and 66% of tibial length. These images were analyzed with *BAMpack* to see what the mean RMS error was for a 2.5 mm axial positioning error, and its effect on internal measurements such as Tb.Dn. Based on this study, it was confirmed that internal measurement comparisons are meaningful as long as the mean RMS value is less than <0.4 mm.

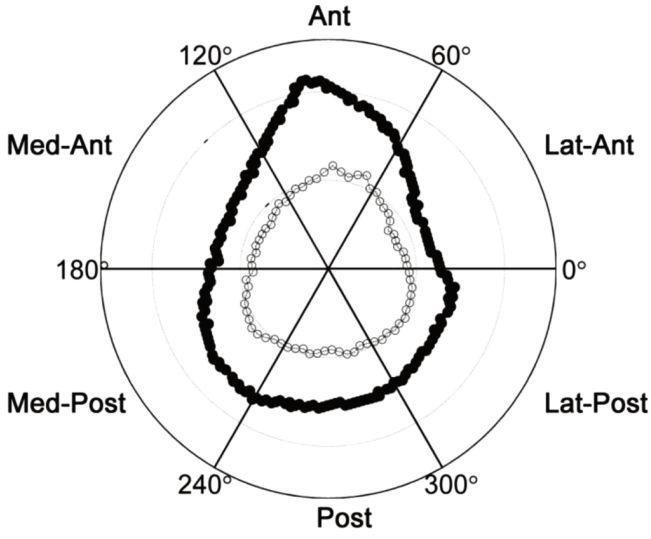


**Figure 1.** Analysis image at the 66% slice of the left tibia, looking proximally, and centered on the intramedullary canal. Closed circles represent the periosteal boundary, and open circles the endosteal boundary. Image was divided into six 60° sectors, as follows, using the positive x-axis as the 0° reference point and moving counter-clockwise. Lateral Anterior (Lat-Ant), Anterior (Ant), Medial Anterior (Med-Ant), Medial Posterior (Med-Post), Posterior (Post), and Lateral Posterior (Lat-Post).

After isolating the tibia from the fibula in each image, each voxel within the tibia was classified based on its density value as being either trabecular (100-600 mg/cm$^3$), transitional (600-800 mg/cm$^3$), or cortical (800-1500 mg/cm$^3$). Histograms for each image indicated there were relatively few pixels in the transitional zone, which is in keeping with the known separation between cortical and trabecular density values.

In addition to calculating cross-sectional parameters of bone mineralization, geometry and strength at each scan site, tissue density, cortical area, and cortical thickness were also calculate by polar region. Images were divided into 36 10° polar sectors, using the positive x-axis as the 0° reference point and moving counter-clockwise. These values were used to visualize the results in polar plots. Statistical analysis, however, was accomplished by calculating values for six 60° polar sectors, as follows: Lateral Anterior (Lat-Ant), Anterior (Ant), Medial Anterior (Med-Ant), Medial Posterior (Med-Post), Posterior (Post), and Lateral Posterior (Lat-Post) (Figure 1).

| | All N=57 | Control N=10 | Aerobic N=14 | Resistance N=16 | Combined N=17 |
|---|---|---|---|---|---|
| **Age (yr)** | 20.1±1.6 | 19.7±1.42 | 21.07±1.90 | 20.06±1.84 | 20.06±1.56 |
| **Height (cm)** | 165.3±6.3 | 165.35±7.04 | 165.46±6.05 | 164.49±7.95 | 164.64±7.14 |
| **Weight (kg)** | 66.0±8.2 | 65.98±8.19 | 64.99±6.79 | 65.03±8.37 | 65.36±12.27 |
| **Body Fat (%)** | 32.3±6.6 | 31.70±9.78 | 33.72±5.48 | 31.23±5.66 | 32.61±6.48 |
| **Tibia Length (mm)** | 352.4±18.7 | 350.7±24.94 | 355.65±15.76 | 353.62±20.63 | 352.35±18.72 |

**Table 1.** Volunteer characteristics (mean±SD).

Volumetric Measures of Bone Mineralization

*Trabecular density, TrDn (mg/cm$^3$).* After converting grayscale values to tissue densities using calibration constants, the average of all voxels falling within the trabecular thresholds (100-600 mg/cm$^3$) were calculated for the entire cross-section and for each 10º and 60º polar sector at the 4% site.

*Cortical density, CtDn (mg/cm$^3$).* After converting grayscale values to tissue densities using calibration constants, the average of all voxels falling within the cortical threshold of 800-2500 mg/cm$^3$ was determined for the entire cross-section and for each 10º and 60º polar sector at both the 38% and 66% sites.

Measures of Bone Geometry

*Total cross-sectional area, TtAr (mm$^2$).* Total cross-sectional area of images taken at the 4%, 38%, and 66% sites was calculated by counting the number of pixels circumscribed by the sub-periosteal boundary, and then multiplying by the image resolution.

*Cortical area, CtAr (mm$^2$).* The areal sum of the voxels in the cortical range was used to determine cortical area (mm$^2$) at the 38% and 66% sites. Calculations were made for each polar sector (e.g., Ct.ArLat-Ant) and for the whole tibial cross section (Ct.ArTot).

*Marrow area, MaAr (mm$^2$).* The areal sum of the voxels circumscribed by the endosteal boundary.

*Tibial diameter (anterior-posterior (AP) and medial-lateral (ML) (mm)).* Diameter of the tibia at the 4%, 38%, and 66% sites was calculated by measuring the distance (mm) from the locations of the voxels at the greatest directional extent in the AP and ML directions.

*Sub-periosteal perimeter, PPm (mm).* Periosteal perimeter was calculated by first identifying the outermost cortical voxels, then smoothing the boundaries by averaging coordinates of neighboring voxels, and then summing the distances between the smoothed boundary voxels.

*Endosteal perimeter, EPm (mm).* Endosteal perimeter was calculated by first identifying the innermost cortical voxels, then smoothing the boundaries as described above.

Measures of Bone Strength

*Cross-sectional area moments of inertia ($I_{AP}$, $I_{ML}$, J, mm$^4$).* Moments of inertia ($I_{AP}$ and $I_{ML}$) were calculated about the anterior-posterior and medial-lateral axes, respectively, as a measure of bending strength independent of the degree of cortical mineralization. The polar moment of inertia ($J= I_{AP}+I_{ML}$) provided a measure of torsional strength. Moments of inertia were calculated at the 38% and 66% sites using only those voxels in the cortical threshold range.

Statistical Analysis

Cross-sectional and sector parameters were analyzed using a repeated measures ANOVA with time (3 time points) and group (4 groups) as factors (SPSS, v15.0, Chicago, IL). Significant time by group interactions were further analyzed using Fisher's LSD post-hoc testing to assess pre-post changes P-value was set at $P \leq 0.05$.

## Results

Of 70 volunteers who consented, 58 completed the study. Of these, the images collected from 1 subject were discarded due to excessive motion artifacts in the image. Included in our final analysis were images from 57 women. Volunteer characteristics are presented in Table 1. All but three volunteers were right leg dominant. There were no between-group differences at baseline for any of the volunteer characteristics.

*Examination of Transitional Zone*

Subcortical pixels comprise about 95% of the bone pixel area at 4% of tibial length, 15% of bone pixel area at 38% of tibial length and 24% of the bone pixel area at 66% of tibial length. Transition zone pixels accounted for 3.5% of subcortical pixels at 4%, 17.9% of subcortical pixels at 38%, and 15.6% of subcortical pixels at 66%. The transitional area, as a percentage of subcortical area, changed less than 1% at all time points and scan locations. In order to make it more likely that the statistical analysis focused on changes derived from true trabecular and true cortical pixels -and not potential partial volume artifacts- we did not include transitional zone pixels in the statistical analysis.

*Volumetric Measures of Bone Mineralization*

Cross-sectional analysis of whole bone at the 4% site yielded a significant time X group interaction for trabecular density, *TrDn* ($p=0.01$). Post-hoc analyses revealed small but significant pre-post increases in *TrDn* for both the aerobic (279.8 to 283.1 mg/cm$^3$, $P<0.001$) and combined (285.1 to 287.5 mg/cm$^3$, $P=0.001$) exercise groups (Table 2).

| | Control (n=10) | | Aerobic (n=14) | | Resistance (n=16) | | Combined (n=17) | |
|---|---|---|---|---|---|---|---|---|
| | **Pre** | **Post** | **Pre** | **Post** | **Pre** | **Post** | **Pre** | **Post** |
| **4% site:** | | | | | | | | |
| Trabecular density (mg/cm$^3$) | 294.2 | 293.8 | 279.8 | **283.1**** | 294.8 | 295.4 | 285.1 | **287.5**** |
| | (12.2) | (12.2) | (37.1) | (36.0) | (37.2) | (36.7) | (24.6) | (22.9) |
| Total cross sectional area (mm$^2$) | 1105.2 | 1093.1 | 1079.2 | 1085.4 | 1055.4 | 1057.7 | 1039.7 | 1039.4 |
| | (98.0) | (100.4) | (117.6) | (114.6) | (136.1) | (146.6) | (106.4) | (114.3) |
| Sub-periosteal perimeter (mm) | 129.3 | 127.6 | 126.9 | 128.2 | 125.3 | 126.3 | 124.1 | 125.6 |
| | (6.0) | (5.9) | (7.3) | (8.2) | (9.5) | (10.3) | (7.0) | (10.2) |
| AP diameter (mm) | 35.4 | 35.2 | 34.6 | 34.7 | 34.0 | 34.0 | 34.3 | 34.4 |
| | (1.9) | (1.9) | (2.2) | (2.2) | (2.2) | (2.5) | (2.3) | (2.6) |
| ML diameter (mm) | 41.2 | 40.5 | 40.9 | 41.4 | 40.3 | 40.3 | 39.5 | 39.5 |
| | (2.5) | (2.4) | (2.8) | (3.2) | (2.5) | (2.5) | (2.4) | (2.5) |
| **38% site:** | | | | | | | | |
| Cortical density (mg/cm$^3$) | 1190.7 | 1190.8 | 1199.3 | 1196.9 | 1198.1 | 1195.7 | 1193.1 | 1191.5 |
| | (18.1) | (18.6) | (15.2) | (18.4) | (18.1) | (16.1) | (13.0) | (13.8) |
| Total cross sectional area (mm$^2$) | 340.1 | 341.8 | 323.4 | **327.2**** | 322.8 | 323.1 | 323.2 | **326.6**** |
| | (40.0) | (40.1) | (34.4) | (36.6) | (39.8) | (38.6) | (33.1) | (33.8) |
| Cortical area (mm$^2$) | 267.6 | 268.5 | 252.9 | 254.8 | 258.5 | 259.5 | 252.3 | 253.3 |
| | (26.6) | (26.0) | (27.2) | (27.7) | (39.3) | (37.6) | (24.8) | (23.3) |
| Marrow area (mm$^2$) | 72.5 | 73.3 | 70.5 | **72.4*** | 64.3 | 63.6 | 70.9 | **73.3**** |
| | (24.4) | (24.5) | (21.3) | (22.3) | (10.4) | (10.8) | (11.5) | (13.4) |
| Sub-periosteal perimeter (mm) | 71.9 | 72.0 | 70.1 | 70.2 | 70.1 | 70.0 | 70.3 | 70.4 |
| | (4.2) | (4.1) | (4.1) | (4.0) | (3.9) | (3.9) | (4.2) | (4.3) |
| Endosteal perimeter (mm) | 35.8 | 36.0 | 36.3 | 36.3 | 34.8 | 34.8 | 36.4 | 36.6 |
| | (4.8) | (5.1) | (5.3) | (5.4) | (2.6) | (2.6) | (3.5) | (3.6) |
| AP diameter (mm) | 25.6 | 25.6 | 24.5 | 24.6 | 25.2 | 25.1 | 24.9 | 25.0 |
| | (1.6) | (1.7) | (1.8) | (1.9) | (1.5) | (1.4) | (2.1) | (2.1) |
| ML diameter (mm) | 19.2 | 19.1 | 19.6 | 19.6 | 18.9 | 19.0 | 19.3 | 19.3 |
| | (1.6) | (1.6) | (1.4) | (1.4) | (1.4) | (1.5) | (1.4) | (1.5) |
| I (AP) (mm$^4$) | 7429 | 7433 | 7329 | 7395 | 6761 | 6852 | 6940 | 6995 |
| | (1799) | (1775) | (1774) | (1821) | (1640) | (1670) | (1639) | (1549) |
| I (ML) (mm$^4$) | 13805 | 14010 | 11934 | 12175 | 12584 | 12560 | 12532 | 12626 |
| | (2871) | (2997) | (2533) | (2692) | (2969) | (2788) | (3209) | (3131) |
| J (mm$^4$) | 21235 | 21443 | 19263 | 19571 | 19346 | 19413 | 19472 | 19621 |
| | (4442) | (4488) | (3913) | (4096) | (4459) | (4331) | (4478) | (4264) |
| **66% site:** | | | | | | | | |
| Cortical density (mg/cm$^3$) | 1162.9 | 1163.1 | 1168.8 | 1169.3 | 1170.8 | 1168.5 | 1167.3 | 1166.2 |
| | (16.4) | (12.8) | (15.9) | (18.9) | (15.6) | (15.9) | (13.3) | (12.2) |
| Total cross sectional area (mm$^2$) | 445.2 | 446.3 | 433.7 | 434.6 | 419.4 | 418.6 | 422.6 | 425.1 |
| | (60.6) | (59.7) | (50.7) | (48.4) | (46.4) | (46.3) | (42.2) | (41.9) |
| Cortical area (mm$^2$) | 295.8 | 294.8 | 281.1 | 280.1 | 290.1 | 289.8 | 285.5 | 286.2 |
| | (29.4) | (30.8) | (31.0) | (32.8) | (38.4) | (36.5) | (26.6) | (25.6) |
| Marrow area | 149.4 | 151.5 | 152.5 | 154.6 | 129.3 | 128.8 | 137.1 | 138.9 |
| | (40.7) | (38.8) | (34.7) | (36.4) | (25.8) | (25.1) | (24.7) | (25.5) |
| Sub-periosteal perimeter (mm) | 86.2 | 85.9 | 84.3 | 84.3 | 82.9 | 82.8 | 83.1 | 83.4 |
| | (5.3) | (5.2) | (5.4) | (5.4) | (4.2) | (4.3) | (4.5) | (4.5) |
| Endosteal perimeter (mm) | 52.3 | 52.8 | 52.9 | 52.9 | 49.5 | 49.4 | 50.4 | 50.6 |
| | (5.8) | (5.4) | (6.1) | (6.2) | (4.7) | (4.8) | (4.3) | (4.3) |
| AP diameter (mm) | 31.7 | 31.7 | 31.2 | 31.3 | 31.5 | 31.5 | 31.0 | 31.2 |
| | (1.6) | (1.5) | (2.2) | (2.2) | (1.7) | (1.7) | (2.1) | (2.1) |
| ML diameter (mm) | 22.1 | 22.1 | 21.9 | 21.9 | 20.9 | 20.9 | 21.4 | 21.5 |
| | (2.3) | (2.5) | (1.7) | (1.8) | (1.9) | (1.9) | (1.7) | (1.7) |
| I (AP) (mm$^4$) | 10842 | 10831 | 10168 | 10139 | 9405 | 9384 | 9733 | 9823 |
| | (3144) | (3082) | (2429) | (2498) | (2377) | (2391) | (2017) | (2037) |
| I (ML) (mm$^4$) | 26628 | 26730 | 24654 | 24545 | 24653 | 24443 | 24101 | 24338 |
| | (4730) | (4810) | (5100) | (5088) | (5036) | (4808) | (5080) | (5114) |
| J (mm$^4$) | 37470 | 37561 | 34822 | 34684 | 34059 | 33827 | 33833 | 34161 |
| | (7642 | (7635) | (7172) | (7148) | (6964) | (6720) | (6622) | (6688) |

*** P<0.01 * P≤ 0.05*

**Table 2.** Cross-sectional parameters (mean (SD)) of bone density, geometry, and strength at sites 4%, 38%, and 66% from the tibial endplate at baseline (pre) and 8 wks (post) following exercise intervention.

| | Control (n=10) | | Aerobic (n=14) | | Resistance (n=16) | | Combined (n=17) | |
|---|---|---|---|---|---|---|---|---|
| | **Pre** | **Post** | **Pre** | **Post** | **Pre** | **Post** | **Pre** | **Post** |
| **4% *TrDn* (mg/cm³)** | | | | | | | | |
| C Lat-Ant | 294.3 | 294.7 | 284.9 | 286.9 | 299.42 | 298.4 | 288.7 | 288.7 |
| | (14.5) | (13.9) | (43.6) | (42.4) | (39.2) | (37.8) | (28.4) | (28.0) |
| Ant | 280.1 | 280.05 | 267.9 | 270.9 | 278.6 | 280.5 | 267.7 | 270.3 |
| | (14.9) | (1.40) | (45.3) | (47.0) | (34.6) | (33.5) | (25.2) | (25.2) |
| Med-Ant | 281.5 | 278.1 | 264.5 | **268.9**** | 274.9 | 274.4 | 269.0 | 270.3 |
| | (23.8) | (19.7) | (36.7) | (36.4) | (35.07) | (35.1) | (20.3) | (17.7) |
| Med-Post | 301.6 | 302.8 | 287.1 | **294.2**** | 295.7 | **301.3**** | 291.6 | **296.1**** |
| | (23.7) | (25.2) | (30.6) | (30.0) | (43.1) | (44.3) | (30.4) | (29.0) |
| Post | 305.9 | 305.6 | 287.5 | 290.0 | 309.6 | 309.3 | 296.8 | 299.7 |
| | (25.8) | (28.4) | (39.4) | (41.2) | (43.6) | (43.9) | (33.4) | (31.4) |
| Lat-Post | 301.2 | 301.9 | 284.2 | 285.0 | 310.0 | 309.2 | 295.7 | 299.0 |
| | (28.5) | (26.2) | (46.4) | (44.2) | (47.2) | (47.4) | (33.1) | (32.5) |
| **38% *CtDn* (mg/cm³)** | | | | | | | | |
| Lat-Ant | 1187.8 | 1185.7 | 1196.8 | 1196.9 | 1198.3 | 1199.1 | 1186.5 | 1187.8 |
| | (14.0) | (14.3) | (20.7) | (21.0) | (17.4) | (16.3) | (17.2) | (14.2) |
| Ant | 1154.3 | 1156.7 | 1163.8 | 1161.4 | 1167.7 | 1165.2 | 1155.8 | 1156.1 |
| | (28.5) | (29.6) | (32.0) | (30.8) | (26.8) | (25.6) | (17.3) | (23.1) |
| Med-Ant | 1192.1 | 1191.8 | 1204.7 | 1205.5 | 1196.6 | 1199.8 | 1198.8 | 1197.0 |
| | (18.3) | (27.7) | (21.1) | (24.1) | (18.1) | (19.8) | (19.2) | (18.3) |
| Med-Post | 1209.9 | 1209.5 | 1216.0 | 1211.6 | 1214.3 | 1208.4 | 1212.5 | 1207.7 |
| | (25.8) | (25.8) | (14.2) | (20.3) | (18.2) | (26.4) | (18.0) | (15.4) |
| Post | 1204.5 | 1199.5 | 1207.0 | 1206.9 | 1201.0 | 1201.1 | 1207.0 | 1203.3 |
| | (21.3) | (21.4) | (20.3) | (21.6) | (22.8) | (19.2) | (20.0) | (21.9) |
| Lat-Post | 1222.0 | 1227.1 | 1232.8 | 1226.2 | 1232.3 | 1223.5 | 1226.0 | 1223.9 |
| | (12.7) | (14.0) | (21.9) | (22.9) | (21.7) | (20.7) | (19.4) | (14.2) |
| **66% *CtDn* (mg/cm³)** | | | | | | | | |
| Lat-Ant | 1139.2 | 1141.4 | 1137.3 | 1137.4 | 1142.6 | 1137.9 | 1143.4 | 1140.5 |
| | (21.4) | (21.4) | (34.5) | (27.6) | (20.6) | (25.9) | (15.4) | (23.9) |
| Ant | 1120.6 | 1127.7 | 1136.1 | 1137.2 | 1137.9 | 1139.4 | 1128.3 | 1128.5 |
| | (35.2) | (29.0) | (27.4) | (35.7) | (24.3) | (27.4) | (22.1) | (20.4) |
| Med-Ant | 1174.1 | 1171.1 | 1185.6 | 1179.7 | 1177.4 | 1166.9 | 1180.4 | 1172.3 |
| | (29.8) | (11.7) | (21.6) | (22.7) | (22.1) | (21.5) | (18.5) | (17.3) |
| Med-Post | 1193.6 | 1185.1 | 1202.8 | 1196.1 | 1200.0 | 1200.8 | 1192.0 | 1197.8 |
| | (21.9) | (20.3) | (16.7) | (38.3) | (15.5) | (21.7) | (21.6) | (14.9) |
| Post | 1193.3 | 1185.5 | 1187.4 | 1185.2 | 1191.2 | 1183.9 | 1194.6 | 1188.6 |
| | (20.1) | (18.5) | (24.4) | (22.4) | (18.0) | (17.2) | (16.7) | (19.6) |
| Lat-Post | 1183.1 | 1190.3 | 1181.6 | 1195.4 | 1191.3 | 1194.0 | 1185.0 | 1189.7 |
| | (34.4) | (19.5) | (15.5) | (16.2) | (23.0) | (19.8) | (14.5) | (16.6) |

***P<0.01 *P≤0.05*

**Table 3.** Regional parameters (mean (SD)) of volumetric bone density (mg/cm³) at sites 4%, 38%, and 66% from the tibial endplate at baseline (pre) and 8 wks (post) following onset of exercise intervention.

Values calculated for each 60° sector are presented in Table 3. Sector analysis revealed significant time X group interactions at the medial aspect of the distal tibia (medial-anterior and medial-posterior sites, P=0.03). Post-hoc analyses of these sectors indicate that pre-post increases in *TrDn* were observed for each exercise condition at the medial-posterior sector (P<0.01), and additionally in the medial-anterior sector in the aerobic group (P<0.01), as depicted in polar plots that represent pre-post analysis for all sectors (Figure 2). Individual percentage changes in *TrDn* in the medial-posterior sector are displayed in Figure 3. The aerobic subject with 11.76% trabecular density increase started with a baseline Med-Post density of 279.12 mg/cm³ versus 287.13 mg/cm³ for her cohort. The Combined group outlier with 8% increase had a baseline density of 238.6 mg/cm³- well below the 291.6 mg/cm³ average for her cohort. These suggest that the combination of low starting trabecular density and impact training may lead to larger increases in trabecular density.

Values for *CtDn* are presented in Table 2. We did not observe significant changes for *CtDn* in whole bone cross-sectional images or at any of the 60° sectors.

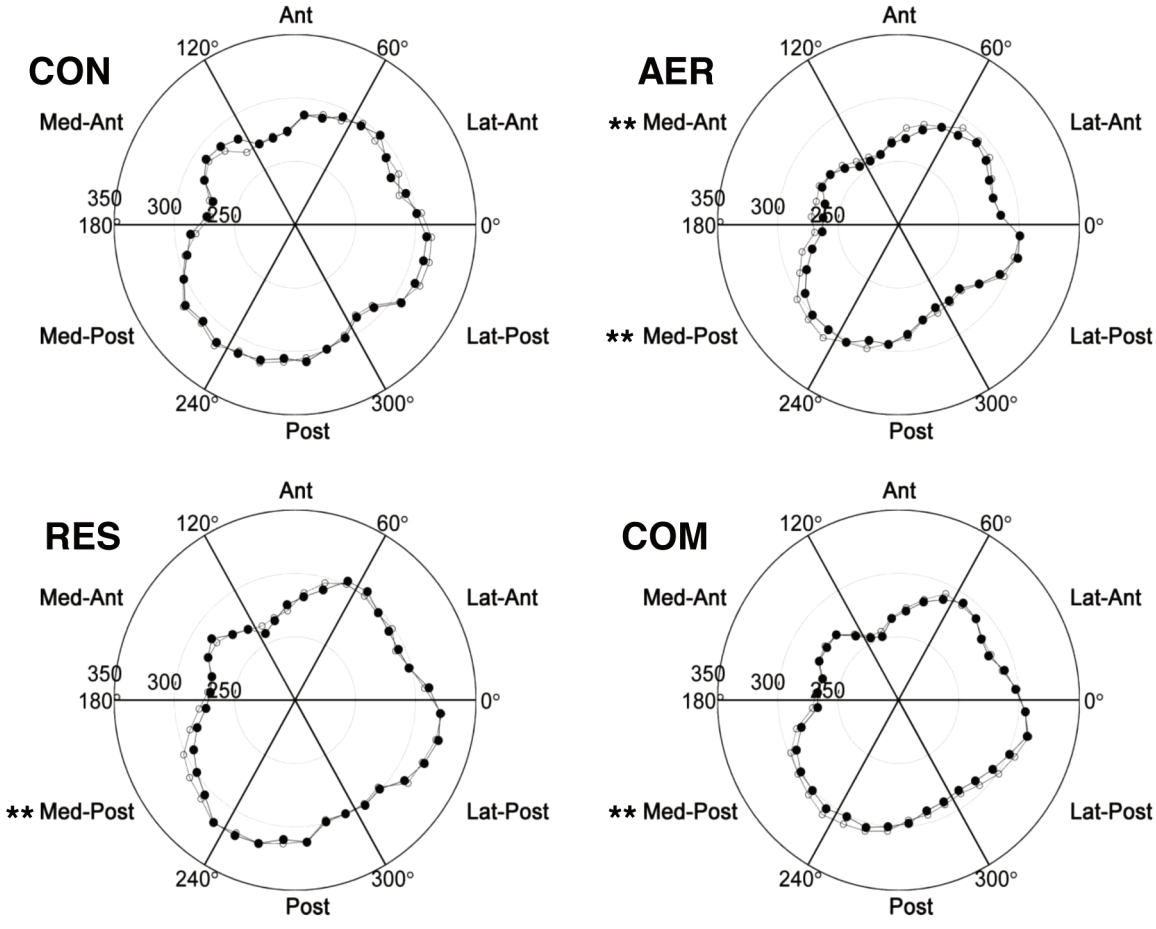


**Figure 2.** Polar plots depicting values for trabecular density at each 10° sector at baseline (closed circles) and after completion of an 8-week exercise intervention (open circles). CON= control group; AER= aerobic training; RES= resistance training; COM= combined aerobic and resistance training. Statistical analysis was conducted at each 60° sector (Lateral Anterior (Lat-Ant), Anterior (Ant), Medial Anterior (Med-Ant), Medial Posterior (Med-Post), Posterior (Post), and Lateral Posterior (Lat-Post)). ** denotes a statistical pre-post difference at annotated sector (P<0.01).

*Measures of Bone Geometry*

Values for geometric measures at the 4, 38, and 66% sites are presented in Table 2. Significant time X treatment interactions were noted at the 38% site for total cross-sectional area (P=0.04) and marrow area (P=0.02), and for AP diameter at the 66% site (P=0.04). Post hoc analyses at the 38% site revealed significant pre-post increase in total cross-sectional area for the AER (P=0.002) and COM (P=0.003) groups. A concomitant pre-post increase in marrow area was observed in the AER (P=0.02) and COM (P=0.001) groups. There were no significant changes for any group for measures of cortical area, sub-periosteal or endosteal perimeters. There were no significant post hoc pre-post changes noted at the 66% site.

*Measures of Bone Strength*

Cross-sectional area moments of inertia ($I_{AP}$, $I_{ML}$, J) are presented in Table 2, and exhibited no significant changes related to exercise intervention.

## Discussion

We developed a pQCT imaging analysis program designed to detect subtle regional changes that might be obscured by whole-image measurements. These changes represent an early bone adaptation response following training programs designed to be osteogenic. Figure 2 clearly visualizes the small but significant increases in *TrDn* at the medial aspect of the ultra-distal tibia (4% site) following 8 cumulative weeks of aerobic, resistance, and combined aerobic and resistance exercise training (distributed over 13 total weeks); no changes occurred in the control group. We also observed increases in total cross-sectional area and marrow area at the distal tibial shaft, however these changes were small, occurred to a minimal extent in the control group, and were not accompanied by changes in sub-periosteal or endosteal perimeter measures.

The increases in *TrDn* at the distal tibia are similar outcomes to animal studies, which found increased trabecular bone mass, thickness and number in cancellous bone of the rat tibia fol-

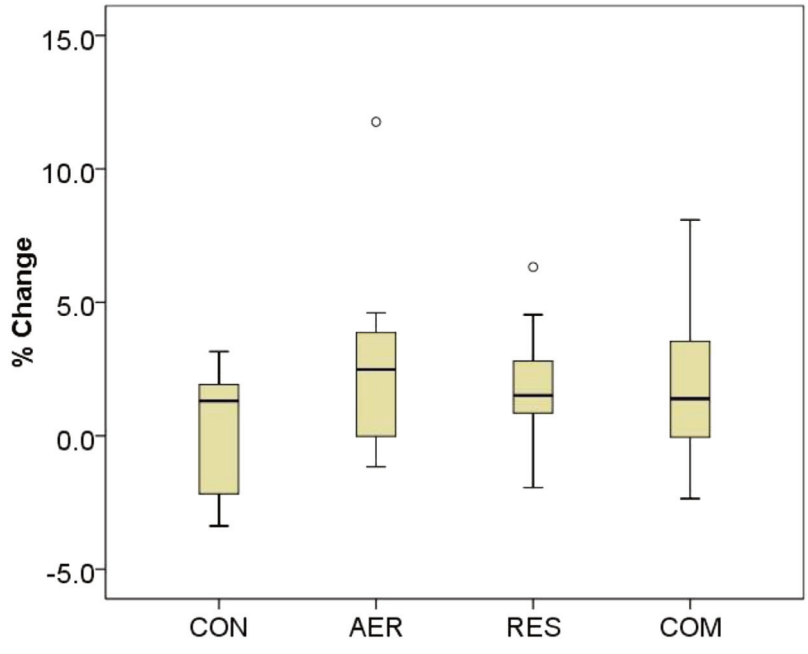


**Figure 3.** Percentage changes in *TrDn* for the Medial-Posterior sector. CON= control group; AER= aerobic training; RES= resistance training; COM= combined aerobic and resistance training.

lowing short-term exercise interventions[3,4]. Our results also agree, in principal, with other studies that have used pQCT in some manner to monitor changes in bone. Findlay et al. found that pQCT of the distal tibia had the potential to be the most sensitive site for measuring morphological changes following tibial fracture[25]. Similarly, Veitch et al. found trabecular bone to be the best sentinel for measuring changes following fracture[26]. This early trabecular modeling is consistent with its faster remodeling rate compared to cortical bone, a fact owed to its greater surface area[27]. Given the appreciably increased mineral density evident in the distal tibia of triple jumper athletes[7] it is conceivable that increased trabecular density could be an early response to exercise intervention. It should also be noted that the control group had a higher baseline *TrDn* (294.2 mg/cm$^3$) than the combined (285.1 mg/cm$^3$), and especially the aerobic (279.8 mg/cm$^3$) group. Starting with lower initial *TrDn* could have predisposed the aerobic and combined groups to greater increases from the intervention. The increase could also have been due tor trabecularization of previously cortical bone, though at the 4% site, there are relatively few voxels which were within cortical thresholds to begin with.

We did not observe changes in *CtDn* at the diaphyseal region of the bone at either the 38% or 66% sites. This would agree with cross-sectional studies indicating that increased *CtDn* is not an expected exercise-induced adaptation. In a study comparing athletes, cortical density has been found similar in jumpers, swimmers, and controls[10]. Even tennis players exhibit similar *CtDn* in the dominant and non-dominant arms[6]. We hypothesized, though did not observe, that any expected beneficial cortical change would be most observable in the anterior sector where density is slightly lower and thus has a greater potential for observable increase. We did observe that the posterior cortex had a higher cortical density than the anterior cortex, both at the 38% and 66% sites, which has been documented previously[21]. Site-specific changes in *CtDn* may be expected primarily in instances of overuse, when extensive remodeling at sites of excessive loading lead to transient decreases in density and bone stress reactions[28]. As our exercise interventions were designed to prevent bone stress injuries, we did not expect to see changes indicative of overuse.

Subtle, significant changes in total cross-sectional area were observed at the 38% site in both aerobic and combined exercise groups, however this was not accompanied by evidence of periosteal expansion through increases in cortical area or sub-periosteal perimeter. This is in contrast to animal studies that evidence significant and observable periosteal perimeter expansion following jump training[29]. It is likely that a more intense and longer duration exercise regimen that incorporates high-impact jumping and sprinting activities would be required to yield similar changes at the diaphysis in humans It is possible that a change in circularity increased the area while preserving the perimeters, but the authors feel a more likely explanation is lack of precision in the perimeter calculation. The approximately 1% increase in total area should have had a concomitant perimeter increase of approximately 0.6%. At the 38% location, this would be 0.4 mm, or 1 additional pixel. Such small changes could easily be obscured by the boundary smoothing technique used to calculate perimeters.

Geometric measures may also be susceptible to "partial volume effects"[30]. This is particularly true at the endosteal and pe-

riosteal boundaries of the diaphysis, and in the trabecular bone that dominates the epiphyses of long bones. Morphological changes will be harder to detect than changes in mineralization due to the number of pixels involved in calculating the changes. While morphological changes depend on changes in the boundary pixels, density changes are calculated from all pixels in the cortical region, of which there are approximately ten times more than the number of boundary pixels. Thus changes in mean values in regional density are based on a much higher number of pixels than changes in cortical thickness, and may more accurately detect subtle changes over the short-term.

Our results suggest that high-impact exercise (i.e., running), as opposed to resistance exercise, is the most effective at producing changes that reflect distal tibial bone adaptation, as suggested by cross-sectional studies comparing athletes with controls[9,31]. During running, muscle forces contribute to posterior-directed loading at the distal tibia during mid-stance, but are directed in an anterior direction during the initial and final phases of the gait cycle[32]. This might explain why the aerobic group, which incorporated a greater volume of running, exhibited increased mineralization at the medial-anterior sector, in addition to the medial-posterior increases noted in all three exercise conditions. That impact exercise seems necessary to produce observable changes is not surprising giving the state of knowledge of bone cell mechanobiology. Dynamic loads are best at producing bone strain rates of sufficient magnitude to produce the interstitial fluid flow that appears necessary to stimulate remodeling[33-35]. For this cohort, the resistance training regimen, while possibly capable of producing high bone strains, may have produced lower strain *rates* than the aerobic regimen.

There are other considerations when looking for short-term, exercise-induced changes in bone. First, since the changes in morphology are subtle, it is important for pre and post images to be registered correctly, lest measurement errors obscure the changes. The main sources of error during image alignment are: 1) having images taken at slightly different locations, 2) movement of the subject during the image collection process which can induce artifacts and 3) improper alignment of pre and post images by the analysis software. If the first two issues are circumvented (in other words, if "clean" images are collected from a subject at the same location) then the software alignment procedure is robust (CV). Second, we acknowledge that increased density assessed using pQCT images provides a surrogate marker of trabecularization, since density changes noted at the 4% site are at the "apparent" level (the average voxel intensity increased). Since each voxel bounded a volume 0.4 mm x 0.4 mm x 2.2 mm, and a typical trabeculae is 0.2 mm thick and 1mm in length, our results suggest that individual trabeculae could have, on average, increased in density, or more likely the trabecular latticework became more tightly packed through apposition to existing or growth of new trabeculae. Finally, as documented elsewhere, pQCT does have limits to its utility[37,38]. It is not calibrated to specifically measure collagen within the bone matrix. As collagen production precedes mineralization in new bone formation, this first step in functional adaptation and remodeling may not be fully captured by pQCT.

In conclusion, use of this pQCT imaging analysis procedure detected subtle, exercise-induced regional increases in trabecular density of the medial distal tibia in young adults, and were most pronounced in the groups incorporating impact exercise. These results suggest that beneficial adaptation of trabecular bone may be an early manifestation of improved bone strength resulting from a well-designed training intervention.

*Acknowledgements*

*The authors thank Heath Isome, Dan Catrambone, and Disa Hatfield for their assistance with data collection and analysis, as well as the volunteers from the University of Connecticut for their time and dedication. We would also like to acknowledge Weixin Shen for providing consultant services during development of the image analysis software. This research was supported, in part, by a grant from the U.S. Army Medical Research and Materiel Command Bone Health and Military Medical Readiness Research Program.*

## References

1. Cullen D, Smith R, Akhter. Time course for bone formation with long-term external mechanical loading. J Appl Physiol 2000;88(6):1943-8.
2. Umemura Y, Ishiko T, Yamauchi T, Kurono M, Mashiko S. Five jumps per day increase bone mass and breaking force in rats. J Bone Miner Res 1997;12(9):1480-5.
3. Westerlind K, Fluckey J, Gordon S, Kraemer W, Farrell P, Turner R. Effect of resistance exercise training on cortical and cancellous bone in mature male rats. J Appl Physiol 1998;84(2):459-64.
4. Bourrin S, Ghaemmaghami F, Vico L, Chappard D, Gharib C, Alexandre C. Effect of a five-week swimming program on rat bone: A histomorphometric study. Calcif Tissue Int 1992;51(2):137-42.
5. Ashizawa N, Nonaka K, Michikami S, Mizuki T, Amagai H, Tokuyama K, et al. Tomographical description of tennis-loaded radius: reciprocal relation between bone size and volumetric BMD. J Appl Physiol 1999;86(4):1347-51.
6. Haapsalo H, Sievanen H, Kannus P, Heinonen A, Oja P, Vuori I. Dimensions and estimated mechanical characteristics of the humerus after long-term tennis loading. J Bone Miner Res 1996;11:864-72.
7. Heinonen A, Sievanen H, Kyrolainen H, Perttunen J, Kannus P. Mineral mass, size, and estimated mechanical strength of triple jumpers' lower limb. Bone 2001;29(3):279-85.
8. Nikander R, Kannus P, Dastidar P, Hannula M, Harrison L, Cervinka T, et al. Targeted exercises against hip fragility. Osteoporos Int 2009;20(8):1321-8.
9. Wilks D, Winwood K, Gilliver S, Kwiet A, Chatfield M, Michaelis I, et al. Bone mass and geometry of the tibia and the radius of master sprinters, middle and long distance runners, race-walkers and sedentary control participants: A pQCT study. Bone 2009;45(1):91-7.
10. Liu L, Maruno R, Mashimo T, Sanka K, Higuchi T,

Hayashi K, et al. Effects of physical training on cortical bone at midtibia assessed by peripheral QCT. J Appl Physiol 2003;95(1):219-24.
11. Vainionpaa A, Korpelainen R, Sievanen H, Vihriala E, Leppaluoto J, Jamsa T. Effect of impact exercise and its intensity on bone geometry at weight-bearing tibia and femur. Bone 2007;40(3):604-11.
12. Turner CH, Robling AG. Designing Exercise Regimens to Increase Bone Strength. Exerc Sport Sci Rev 2003; 31(1):45-50.
13. Lester M, Urso M, Evans RK, Pierce J, Spiering B, Maresh C, et al. Influence of exercise mode and osteogenic index on bone biomarker responses during short-term physical training. Bone 2009;45(4):768-76.
14. Fujita T. Volumetric and projective bone mineral density. J Musculoskelet Neuronal Interact 2002;2(4):302-5.
15. Sievanen H, Koskue V, Rauhio A, Kannus P, Heinonen A, Vuori I. Peripheral quantitative computed tomography in human long bones: evaluation of *in vitro* and *in vivo* precision. J Bone Miner Res 1998;13(5):871-82.
16. Heinonen A, Sievanen H, Kannus P, Oja P, Pasanen M, Vuori I. High-impact exercise and bones of growing girls: a 9-month controlled trial. Osteoporos Int 2000;11(12):1010-7.
17. Johannsen N, Binkley T, Englert V, Neiderauer G, Specker B. Bone response to jumping is site-specific in children: a randomized trial. Bone 2003;33(4):533-9.
18. Macdonald HM, Kontulainen SA, Khan KM, McKay HA. Is a school-based physical activity intervention effective for increasing tibial bone strength in boys and girls? J Bone Miner Res 2007;22(3):434-46.
19. Specker B, Binkley T. Randomized trial of physical activity and calcium supplementation on bone mineral content in 3- to 5-year-old children. J Bone Miner Res 2003; 18(5):885-92.
20. Nonaka K, Fukuda S, Aoki K, Yoshida T, Ohya K. Regional distinctions in cortical bone mineral density measured by pQCT can predict alterations in material property at the tibial diaphysis of the Cynomolgus monkey. Bone 2006;38(2):265-72.
21. Lai YM, Qin L, Hung VW, Chan KM. Regional differences in cortical bone mineral density in the weight-bearing long bone shaft - a pQCT study. Bone 2005;36(3):465-71.
22. Lai YM, Qin L, Yeung HY, Lee KK, Chan KM. Regional differences in trabecular BMD and micro-architecture of weight-bearing bone under habitual gait loading - a pQCT and microCT study in human cadavers. Bone 2005; 37(2):274-82.
23. Cheng S, Sipila S, Taaffe DR, Puolakka J, Suominen H. Change in bone mass distribution induced by hormone replacement therapy and high-impact physical exercise in post-menopausal women. Bone 2002;31(1):126-35.
24. Evans RK, Negus C, Antczak AJ, Yanovich R, Israeli E, Moran DS. Sex differences in parameters of bone strength in new recruits: beyond bone density. Med Sci Sports Exerc 2008;40(11Suppl):S645-53.
25. Findlay SC, Eastell R, Ingle BM. Measurement of bone adjacent to tibial shaft fracture. Osteoporos Int 2002; 13(12):980-9.
26. Veitch SW, Findlay SC, Hamer AJ, Blumsohn A, Eastell R, Ingle BM. Changes in bone mass and bone turnover following tibial shaft fracture. Osteoporos Int 2006; 17(3):364-72.
27. Guo X. Mechanical Properties of cortical bone and cancellous bone tissue. In: Cowin S, editor. Bone MEchanics Handbook, 2nd Edition. Boca Raton, FL: CRC Press; 2001. p. 1-23.
28. Magnusson H, Westlin N, Nyquist F, Gardsell P, Seeman E, Karlsson M. Abnormally decreased regional bone density in athletes with medial tibial stress syndrome. Amer J Sports Med 2001;29(6):712-5.
29. Umemura Y, Nagasawa S, Honda A, Singh R. High-impact exercise frequency per week or day for osteogenic response in rats. J Bone Miner Metab 2008;26(5):456-60.
30. Stratec Medizintechnik G. XCT 3000 Manual Software version 5.50 2004.
31. Nikander R, Sievanen H, Heinonen A, Kannus P. Femoral neck Structure in Adult Female Athletes Subjected to Different Loading Modalities. J Bone Miner Res 2005; 20:520-528.
32. Sasimontonkul S, Bay BK, Pavol MJ. Bone contact forces on the distal tibia during the stance phase of running. J Biomech 2007;40(15):3503-9.
33. Turner CH, Owan I, Takano Y. Mechanotransduction in bone: told of strain rate. Amer J Physiol 1995;269(3 Pt.1):E438-42.
34. Mosley JR, Lanyon LE. Strain rate as a controlling influence on adaptive modeling in response to dynamic loading of the ulna in growing male rats. Bone 1998;23(4):313-8.
35. Han Y, Cowin S, Schaffler MB, Weinbaum S. Mechanotransduction and strain amplification in osteocyte cell processes. Proc Nat Acad Sci USA 2004;101(47):16689-94.
36. Kraemer W, Patton J, Gordon S, Harman E, Deschenes M, Reynold K, et al. Compatibility of high-intensity strength and endurance training on hormonal and skeletal muscle adaptations. J Appl Physiol 1995;78(3):976-89.
37. Ferretti J. Noninvasive Assessment of Bone Architecture and Biomechanical Properties in Animals and Humans Employing pQCT Technology. J Jpn Soc Bone Morphometry 1997;7:115-25.
38. Ferretti J, Cointry G, Capozza R. Noninvasive Analysis of Bone Mass, Structure, and Strength. In: Yuehuei H, editor. Orthopaedic Issues in Osteoporosis. Boca Raton, FL: CRC Press; 2002. p. 145-167.